ACS SyntheticBiology

pubs.acs.org/synthbio

Research Article

Self-Sufficient In Vitro Multi-Enzyme Cascade for Efficient Synthesis of Danshensu from L-DOPA

Ruizhi Han,[#] Ke Gao,[#] Yulin Jiang, Jieyu Zhou, Guochao Xu, Jinjun Dong, Ulrich Schwaneberg, Yu Ji,* and Ye Ni*

Cite This: *ACS Synth. Biol.* 2023, 12, 277−286

Read Online

ACCESS | Metrics & More | Article Recommendations | Supporting Information

ABSTRACT: Danshensu (DSS), a traditional Chinese medicine, is widely used for the treatment of cardiovascular and cancer diseases. Here, a one-pot multi-enzyme cascade pathway was designed for DSS synthesis from L-DOPA using tyrosine aminotransferase from *Escherichia coli* (*Ec*TyrB) and D-isomer-specific 2-hydroxyacid dehydrogenase from *Lactobacillus frumenti* (*Lf*D2-HDH). Glutamate dehydrogenase from *Clostridium difficile* (*Cd*gluD) was also introduced for a self-sufficient system of α-ketoglutaric acid and NADH. Under optimal conditions (35 °C, pH 7.0, *Ec*TyrB:*Lf*D2-HDH:*Cd*gluD = 3:2:1, glutamate:NAD^+ = 1:1), 98.3% yield (at 20 mM L-DOPA) and space-time yield of 6.61 g L^{-1} h^{-1} (at 40 mM L-DOPA) were achieved. Decreased yields of DSS at elevated L-DOPA concentrations (100 mM) could be attributed to an inhibited *Cd*gluD activity caused by NH_4^+ accumulation. This developed multi-enzyme cascade pathway (including *Ec*TyrB, *Lf*D2-HDH, and *Cd*gluD) provides an efficient and sustainable approach for the production of DSS from L-DOPA.

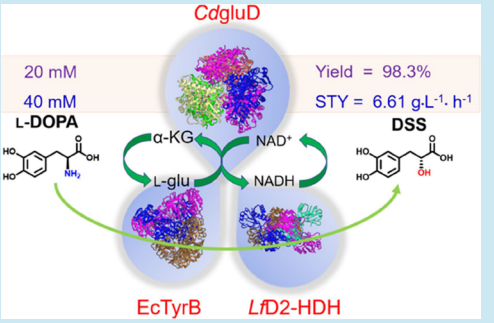

KEYWORDS: *Danshensu, L-DOPA, multi-enzyme cascade, self-sufficient, one-pot*

INTRODUCTION

Danshensu (3,4-dihydroxyphenyllactic acid, DSS), as one of the most important water-soluble components in *Salvia miltiorrhiza* (danshen, traditional Chinese medicine), is widely employed in the treatment of angina pectoris and other cardiovascular diseases.[1,2] For instance, DSS can offer significant cardioprotective effect from myocardial ischemia/reperfusion injury,[3] efficacious anti-ischemic and anti-atherosclerosis effect,[4] and protective effect from doxorubicin-induced cardiotoxicity.[5] In addition, DSS has some other important pharmacological functions, such as neuroprotectant,[6] antioxidant,[7,8] anti-tumor,[9] anti-platelet aggregation agents,[10] anti-osteogenic,[11] and vision protection.[12]

DSS is mainly produced by physical extraction, chemical synthesis, or biosynthesis. Physical extraction is the traditional method for DSS production (mainly from natural plant *S. miltiorrhiza*).[13] The scarce resource of *S. miltiorrhiza*, as well as dissatisfactory yield and purity of DSS, limit the natural plant extraction of DSS to meet industrial requirement.[14] Therefore, chemical synthesis routes with classical Knoevenagel condensation[15] and Darzens condensation[16] gradually advance as alternative methods for DSS production. Although chemical synthesis approaches ease the limitation of *S. miltiorrhiza*, problems of poor chiral selectivity and laborious steps are inextricable.[17] Recently, chemical-enzymatic synthesis and biosynthesis methods for the production of DSS has attracted more attention. For instance, DSS was synthesized from 3,4-dihydroxybenzaldehyde and acetylglycine catalyzed by resting cells of *Pediococcus acidilactici* 1.2696, leading to 70.5% yield and 0.69 g L^{-1} DSS.[18] By employing a coenzyme-nonspecific D-lactate dehydrogenase from *Lactobacillus reuteri*, enzymatic synthesis of DSS from 3,4-dihydroxyphenylpyruvic acid (DPA) resulted a yield of 95.4% and 1.89 g L^{-1}[19] L-DOPA as a cost-effective compound, is an alternative for expensive 3,4-dihydroxyphenylpyruvic acid.[20] L-DOPA was employed for the production of DSS by enzymatic catalysis using L-amino acid oxidase from *Crotalus adamanteus*, and D-lactate dehydrogenase (LDH) from *Lactobacillus leishmannii*.[21] Furthermore, an engineered *Escherichia coli* strain co-expressing L-amino acid deaminase (AADL), LDH, and L-glutamate dehydrogenase (GDH) was constructed for DSS production from L-DOPA, and 95% yield was achieved via whole-cell biotransformation.[22] Up to now, based on our knowledge, this method is the most promising approach reported for the production of DSS (high yield and cheap substrate L-DOPA). However, the low catalytic efficiency

Received: October 18, 2022
Published: November 22, 2022

https://doi.org/10.1021/acssynbio.2c00552
ACS Synth. Biol. 2023, 12, 277−286

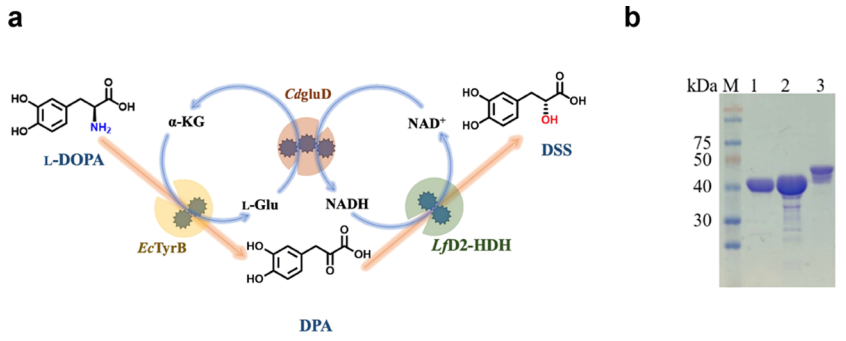

Figure 1. (a) In vitro multi-enzyme route designed for DSS synthesis from L-DOPA (DPA: 3,4-dihydroxyphenylpyruvic acid; α-KG: α-ketoglutaric acid; *Ec*TyrB: aromatic amino acid aminotransferase; *Lf*D2-HDH: D-isomer specific 2-hydroxyacid dehydrogenase; *Cd*gluD: glutamate dehydrogenase). (b) SDS-PAGE analysis of various recombinant proteins (Lane M: protein marker; 1: *Ec*TyrB, 2: *Lf*D2-HDH; 3: *Cd*gluD).

Table 1. Information of Enzymes Used in this Study

enzyme	GenBank accession no	source	specific activity (U/mg)[a]	$\Delta G'^{\circ}$[b] (kJ/mol)	K'_{eq}[b]
aromatic amino acid aminotransferase (*Ec*TyrB)	ACT45717	*E. coliBL21*	0.31	−8.20	30.0
D-isomer specific 2-hydroxyacid dehydrogenase (*Lf*D2-HDH)	KRL27985.1	*L. frumenti*	14.3	−19.5	2.71×10^3
glutamate dehydrogenase (*Cd*gluD)	AAA62756.1	*C. difficile*	0.14	36.5	4.02×10^{-7}

[a]Specific activity was determined using purified enzymes. [b]$\Delta G'^{\circ}$ and K'_{eq} were obtained from http://equilibrator.weizmann.ac.il/.

(space-time yield = 1.96 g L^{-1} h^{-1}) caused by the low mass transfer of whole-cell catalysis still needs improvement.

In vitro multi-enzyme (cell-free) cascade reaction is regarded as a potential next-generation biomanufacture platform, which is composed of multiple enzymes and/or coenzymes under complicated reactions.[23−26] In vitro enzymatic bioreaction systems display many advantages such as near-theoretical product yield, efficient mass transfer, and unprecedented engineering possibilities.[27−29]

Aromatic amino aminotransferase (AroAT, EC 2.6.1.57), one typical pyridoxal 5-phosphate (PLP)-dependent enzyme, is an important enzyme in the biosynthesis of aromatic amino acids.[30] Tyrosine aminotransferase (TyrB), as one important AroAT, could catalyze transamination between aromatic amino acid and α-ketoglutaric acid (α-KG).[31,32] For instance, TyrB was used to produce 3,4-dihydroxyphenylpyruvic acid (DPA) from L-DOPA with α-KG and L-glutamate as the donor and acceptor, respectively.[21] D-Isomer-specific 2-hydroxyacid dehydrogenase (D2-HDH, EC1.1.1) is a NADH/NADPH-dependent reductase, which can catalyze reduction of 2-keto acid to 2-hydroxy acid with NADH as a cofactor.[33] NADH and NADPH, as the most commonly used cofactors in the redox reaction,[34] are not cost-effective for industrial applications. Although glucose dehydrogenase (GDH)[35,36] and formic dehydrogenase (FDH)[37,38] are usually coupled with oxidoreductase for the regeneration of NADH/NADPH, a large amount of additional by-substrates (glucose and formic acid) are required and the by-products (gluconic acid and CO_2) often affect the catalytic efficiency and product purity.

In this study, an in vitro multi-enzyme cascade route catalyzed by TyrB from *E. coli* (*Ec*TyrB) and D2-HDH from *Lactobacillus frumenti* (*Lf*D2-HDH) was designed for producing DSS from L-DOPA. Glutamate dehydrogenase from *Clostridium difficile* (*Cd*gluD) was introduced to simultaneously realize the regeneration of NADH and α-KG, which are essential as a cofactor and cosubstrate in this cascade reaction. Furthermore, optimization of reaction conditions was performed for the enhanced DSS yield using 10 mM L-DOPA. Under optimal conditions, multi-enzyme cascade synthesis of DSS from elevated concentrations of L-DOPA was investigated, and the reason for significantly decreased yield of DSS from 100 mM was explored. This newly designed one-pot multi-enzyme cascade is featured with facile preparation, low cost, and high efficiency, providing a promising biocatalytic approach for the production of DSS.

RESULTS

Designing an In Vitro Multi-Enzyme Cascade Route for the Production of DSS from L-DOPA. An in vitro multi-enzyme cascade for DSS production from L-DOPA was designed using *Ec*TyrB, *Lf*D2-HDH, and *Cd*gluD in this study (Figure 1a). This route consists of three enzymatic reactions: first, L-DOPA is deaminated by *Ec*TyrB to produce DPA, and α-KG acts as an amino acceptor to generate glutamate; Then, DPA is converted to DSS by *Lf*D2-HDH using NADH as a cofactor; finally, NADH and α-KG are regenerated from NAD^+ and glutamate by the recycling reaction catalyzed by *Cd*gluD, *Ec*TyrB and *Cd*gluD that were employed as the optimal enzymes for the reactions (1) and (3), respectively, based on previous reports.[39−41] Because DSS is generated by the reduction of DPA catalyzed by LDH/HDH according to reaction (2),[21,22,33] the efficacy of DSS synthesis mostly depends on the catalytic activity of LDH/HDH. Here, the recombinant LDHs and HDHs from different microorganisms (e.g., *L. reuteri*, *L. secaliphilu*, *L. rossiae*, *L. lactis*, *Weissella cryptocercid*, *L. oeni*, and *L. frumenti*)[18,42,43] were expressed and evaluated. As shown in Figure S1, D2-HDH from *L. frumenti* (*Lf*D2-HDH) and LDHs from *L. rossiae*, *L. frumenti*, and *L. secaliphilu* showed more soluble expression than other LDHs from *W. cryptocercid*, *L. lactis*, *L. oeni*, and *L. reuteri*. Activities of their crude enzymes were also investigated and *Lf*D2-HDH displayed the highest activity (69.6 mU·mg^{-1}, Table S1). Therefore, *Lf*D2-HDH was selected as the best candidate for reaction (2) because of its easy soluble expression and high activity. The standard Gibbs free energy change ($\Delta G'^{\circ}$) of *Ec*TyrB and *Lf*D2-HDH were evaluated

https://doi.org/10.1021/acssynbio.2c00552
ACS Synth. Biol. 2023, 12, 277−286

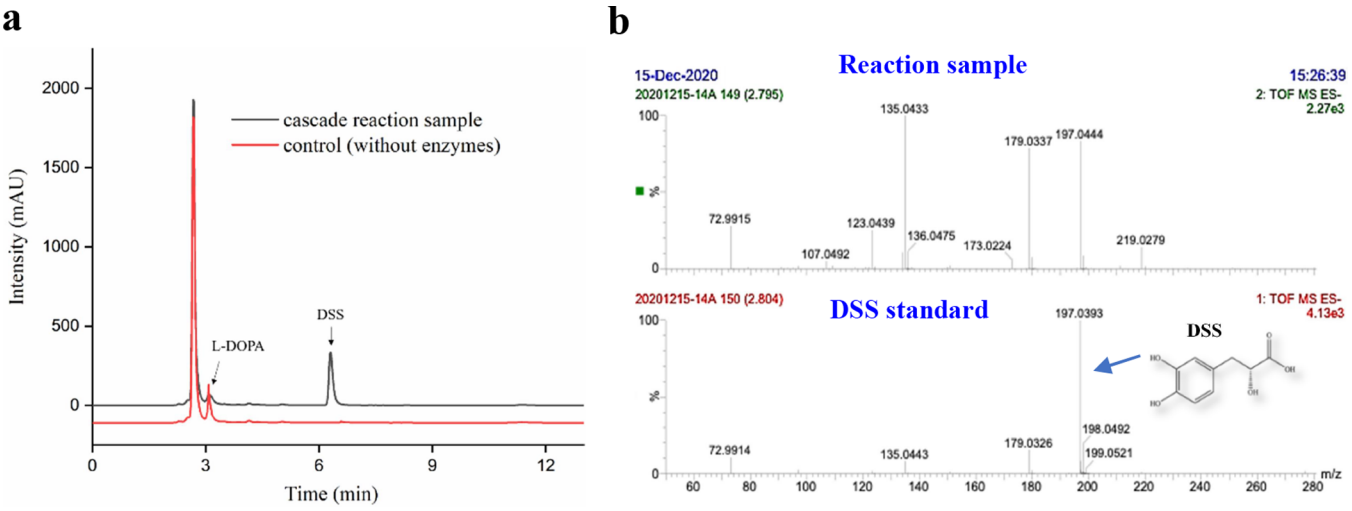

Figure 2. Identification of DSS synthesis. (a) HPLC analysis of DSS synthesized from L-DOPA. (b) LC−MS analysis of the multi-enzyme cascade reaction as proof of DSS production.

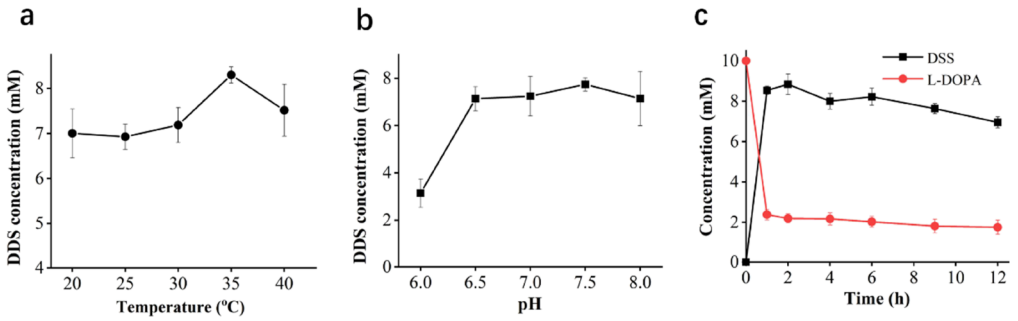

Figure 3. Effect of reaction (a) temperature, (b) pH, and (c) time on DSS production in the multi-enzyme cascade reaction. (a) Ten milliliter reaction containing 10 mM L-DOPA, 10 mM NAD^+, 10 mM glutamate, and 0.1 U/mL of each enzyme in 50 mM PBS buffer (pH 7.0) was performed at 20−40 °C for 2 h. (b) Ten milliliter reaction containing 10 mM L-DOPA, 10 mM NAD^+, 10 mM glutamate, and 0.1 U/mL of each enzyme in various 50 mM PBS buffers (pH 6.0−8.0) was performed at 35 °C for 2 h. (c) Ten milliliter reaction containing 10 mM L-DOPA, 10 mM NAD^+, 10 mM glutamate, 0.1 U mL^{-1} *Ec*TyrB, 0.1 U mL^{-1} *Lf*D2-HDH, and 0.1 U mL^{-1} *Cd*gluD in 50 mM PBS buffer (pH 7.0) was performed at 35 °C. Values are means of triplicate determinations.

(−8.2 and −19.5 kJ/mol, Table 1), suggesting that the entire biocatalytic route for DSS production is thermodynamically favorable. Although the $\Delta G'^{\circ}$ of *Cd*gluD (36.5 kJ/mol) is thermodynamically unfavorable, it only participates in cofactor regeneration and will not hamper DSS synthesis. The reaction equilibrium constants (K'_{eq}) values of *Ec*TyrB (30) and *Lf*D2-HDH (2.71×10^3) further suggest the potential high conversion of DSS using this cascade route (Table 1).

All selected enzymes were purified by a nickel column and analyzed by sodium dodecyl sulfate-polyacrylamide gel electrophoresis (SDS-PAGE), and more than 90% purity of *Ec*TyrB, *Lf*D2-HDH, and *Cd*gluD were obtained. Their molecular weights were about 43, 40, and 46 kDa, respectively (Figure 1b). The specific activities of purified *Ec*TyrB, *Lf*D2-HDH, and *Cd*gluD were determined to be 0.31, 14.3, and 0.14 U mg^{-1}, respectively (Table 1).

Identification of DSS Synthesis by the In Vitro Multi-Enzyme Cascade Route. One-pot cascade reaction by multi-enzymes (purified *Ec*TyrB, *Lf*D2-HDH, and *Cd*gluD) was performed and the products/by-products were determined by high-performance liquid chromatography (HPLC). To identify the product and by-products, a suitable HPLC method was optimized and the standard curves of DSS (6.36 min), L-DOPA (3.31 min), and DPA (8.38 min) were also established (Figure S2). As shown in Figure 2a, compared with the control, the sample of the cascade reaction displayed one product peak at the retention time of 6.36 min, which is in accordance with the DSS standard (Figure S2). Furthermore, liquid chromatography−mass spectrometry (LC−MS) analysis confirmed that m/z ratio 197 is consistent with that of the DSS standard (Figure 2b). Therefore, these results confirm that DSS can be produced from L-DOPA via this newly designed in vitro multi-enzyme cascade route.

Optimization of Reaction Conditions for DSS Production. *Optimization of Reaction Temperature, pH, and Time.* The effect of reaction temperature, pH, and reaction time were evaluated with 10 mM L-DOPA. As shown in Figure 3a, the titer of DSS remained relatively constant over the temperature range of 20−40 °C. The optimal reaction temperature for DSS production was determined to be 35 °C, and the DSS titer at 40 °C still kept more than 88% of that at 35 °C. In addition, reaction pH was also optimized. The DSS titer remained relatively stable with the range of pH 6.5−8.0 and reached the highest at pH 7.5 (Figure 3b). Although a slight decrease (about 7%) was observed at pH 7.0, it was selected as the optimum pH for DSS production because of better stability of DSS at neutral pH. Time course of the cascade reaction was monitored to investigate the effect of

https://doi.org/10.1021/acssynbio.2c00552
ACS Synth. Biol. 2023, 12, 277−286

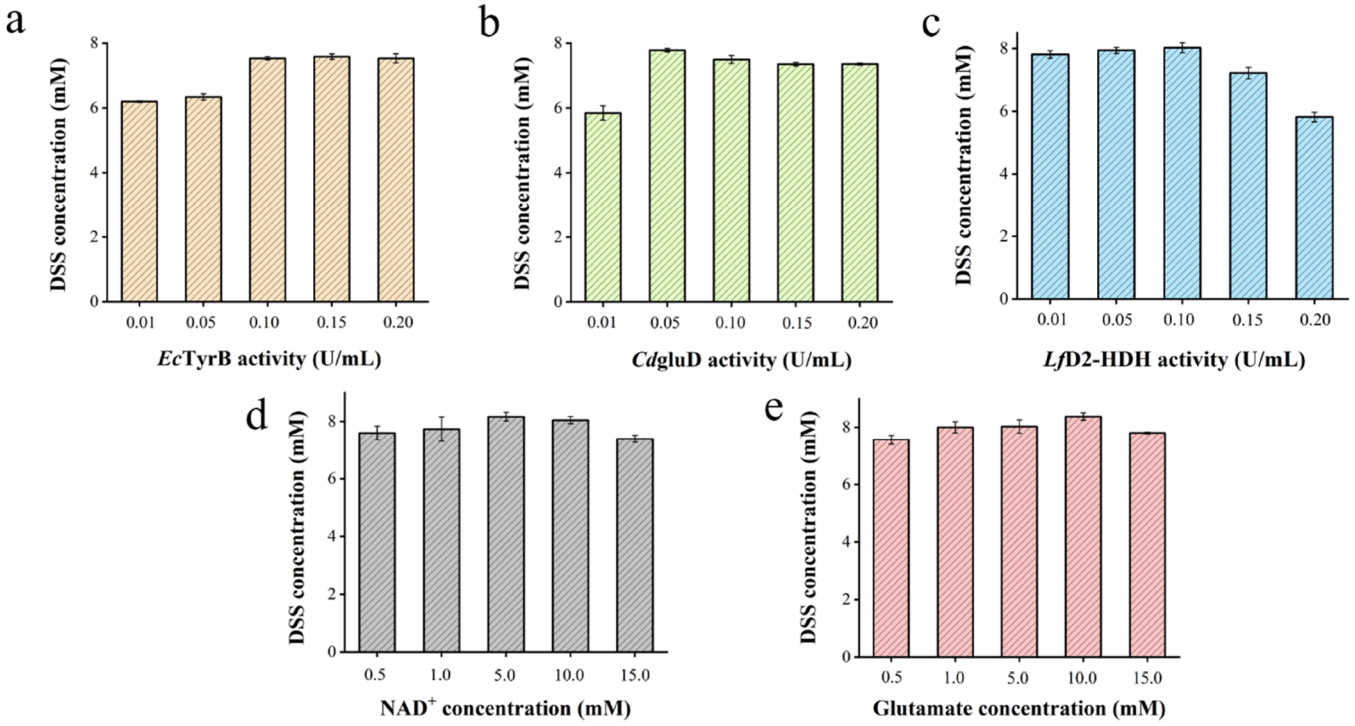

Figure 4. Optimization of enzyme loadings and cofactor concentration for DSS production in multi-enzyme cascade reactions. (a) Effect of *Ec*TyrB loading: 0.01−0.20 U mL^{-1}*Ec*TyrB, 0.1 U mL^{-1} of the other two enzymes. (b) Effect of *Cd*gluD loading: 0.01−0.20 U mL^{-1}*Cd*gluD, 0.15 U mL^{-1} of *Ec*TyrB, and 0.1 U mL^{-1} of *Lf*D2-HDH. (c) Effect of *Lf*D2-HDH loading: 0.01−0.20 U mL^{-1}*Lf*D2-HDH, 0.15 U mL^{-1} of *Ec*TyrB, and 0.05 U mL^{-1} of *Cd*gluD. (d) Effect of NAD^+: 0.5−15 mM NAD^+, 10 mM glutamate. (e) Effect of glutamate: 0.5−15 mM glutamate, 5 mM NAD^+. All reaction mixtures (10 mL) contained 10 mM L-DOPA in 50 mM PBS buffer (pH 7.0) and were performed at 35 °C for 2 h. Values are means of triplicate determinations.

reaction time on DSS accumulation. The highest DSS concentration of 8.9 mM was obtained from 10 mM L-DOPA at 2 h (Figure 3c). After 2 h, the concentration of DSS gradually decreased as the reaction proceeded. As shown in Figure S3, a gradual accumulation of by-product DPA was also observed as DSS decreased (especially after 9 h).

Optimization of Loadings of EcTyrB, LfD2-HDH, CdgluD, NAD^+, and Glutamate. To optimize the loadings of each enzyme (*Ec*TyrB, *Lf*D2-HDH, and *Cd*gluD) and additional NAD^+ and glutamate, the cascade reaction was performed with 10 mM L-DOPA. As shown in Figure 4a, the DSS concentration was enhanced from 6.19 to 7.58 mM when the loading *of Ec*TyrB increased from 0.01 to 0.10 U mL^{-1} and remained similar at higher *Ec*TyrB loadings of 0.10−0.20 U mL^{-1}. The highest DSS concentration of 7.59 mM was achieved with 0.15 U mL^{-1}*Ec*TyrB. For *Cd*gluD, the DSS concentration reached the highest of 7.78 mM at 0.05 U mL^{-1}*Cd*gluD, and further enhanced *Cd*gluD loading had no positive effect on DSS accumulation (Figure 4b). Therefore, the loading of *Lf*D2-HDH was optimized based on 0.15 U mL^{-1}*Ec*TyrB and 0.05 U mL^{-1}*Cd*gluD. As shown in Figure 4c, the highest concentration of DSS of 8.02 mM was achieved at 0.10 U mL^{-1}*Lf*D2-HDH. As a result, the optimal enzyme loading ratio of *Ec*TyrB, *Lf*D2-HDH, and *Cd*gluD were determined to be 3:2:1.

NAD^+ and glutamate are an important cofactor and cosubstrate in the cascade process for DSS synthesis. The initial concentrations of NAD^+ and glutamate were optimized under above optimized temperature, pH, and enzyme loadings. As shown in Figure 4d, the highest DSS concentration of 8.16 mM was obtained with 5 mM NAD^+, and further increased NAD^+ caused a decrease in DSS accumulation. For glutamate, the concentration of DSS increased to the highest level of 8.39 mM with enhanced glutamate addition from 0.5 to 10 mM (Figure 4e). Therefore, the optimum concentrations of NAD^+ and glutamate were 5 and 10 mM, respectively.

Based on the above analysis, the optimal conditions for the cascade reaction with 10 mM L-DOPA were as follows: 10 mL mixture including 50 mM phosphate buffer saline (PBS) buffer (pH 7.0), 5 mM NAD^+, 10 mM glutamate, 0.15 U mL^{-1}*Ec*TyrB, 0.10 U mL^{-1}*Lf*D2-HDH, and 0.05 U mL^{-1}*Cd*gluD at 35 °C. Under above optimum conditions, 9.20 mM of DSS was obtained from 10 mM L-DOPA at 2 h with a space−time yield of 1.82 g L^{-1} h^{-1} (Table 2).

In Vitro Multi-Enzyme Cascade Synthesis of DSS and Whole-Cell Reaction from Elevated Concentrations of L-DOPA. Elevated concentrations of L-DOPA were attempted in this multi-enzyme cascade. Based on optimal reaction conditions, double loadings of enzymes and cofactors were employed as follows, including 10 mM NAD^+, 20 mM glutamate, and enzyme loadings of 0.3 U mL^{-1}*Ec*TyrB, 0.2 U mL^{-1}*Lf*D2-HDH, and 0.1 U mL^{-1}*Cd*gluD. As shown in Table 2, with the increasing of L-DOPA from 20 to 50 mM, although the yield of DSS decreased from 98.3 to 82.8%, the ratio of substrates/catalysts (S/C) gradually increased from 0.86 to 2.26, respectively. The highest space−time yield of 6.61 g L^{-1} h^{-1} was reached at 40 mM L-DOPA and decreased to 4.09 and 2.45 at 50 and 100 mM L-DOPA, respectively.

The recombinant *E. coli* BL21(DE3) strain harboring plasmids pRSFDuet1/*Ec*TyrB/*Lf*D2-HDH and pETDuet1/*Cd*gluD was constructed. As shown in Figure S5a, *Cd*gluD exhibited a mass of soluble expression, whereas enzymes

https://doi.org/10.1021/acssynbio.2c00552
ACS Synth. Biol. 2023, 12, 277−286

Table 2. DSS Production from L-DOPA in Multi-Enzyme Cascade Reactions

L-DOPA/mM	yield[a]	DSS/mM	space-time yield[b]/g L^{-1} h^{-1}	enzyme loadings[c]/mg	S/C[d]
10	92.0%	9.20	1.82	22.5	0.81
20	98.3%	19.7	3.89	45.0	0.86
30	93.5%	28.1	5.56	45.0	1.23
40	83.7%	33.5	6.61	45.0	1.47
50	82.8%	41.4	4.09	45.0	1.81
100	51.5%	51.5	2.54	45.0	2.26

[a] yield = $\frac{\text{produced DSS concentration}}{\text{initial L-DOPA concentration}}$. [b] Space − time yield = $\frac{\text{produced DSS concentration}}{\text{reaction time}}$. [c] Enzyme loadings: 10 mL of the reaction mixture with 10 mM L-DOPA including 0.15 U mL^{-1}*Ec*TyrB, 0.1 U mL^{-1}*Lf*D2-HDH, and 0.05 U mL^{-1}*Cd*gluD, and the total mass of all three enzymes (lyophilized crude enzyme powder) was 22.5 mg; 10 mL of the reaction mixture with more than 20 mM L-DOPA including 0.3 U mL^{-1}*Ec*TyrB, 0.2 U mL^{-1}*Lf*D2-HDH, and 0.1 U mL^{-1}*Cd*gluD, and the total mass of all three enzymes (lyophilized crude enzyme powder) was 45 mg. [d] S/C = $\frac{\text{amount of L-DOPA converted}}{\text{amount of enzymes}}$.

*Ec*TyrB and *Lf*D2-HDH showed slight soluble expression. HPLC analysis displayed that no DSS product was synthesized in the whole-cell reaction within the whole range of 0−24 h (Figure S5b). However, the peak area at 8.38 min (DPA) was gradually decreased within the range of 2−8 h and that at 8.76 min, the unknown compound was gradually increased after 12 h.

Analysis for Decreased DSS Yield at 100 mM L-DOPA. To investigate the reason for decreased yield and space−time yield of DSS at 100 mM L-DOPA, different strategies were performed as follows. The substrate inhibition effect was explored first because of the low solubility of L-DOPA. As shown in Figure 5, when 197 mg of L-DOPA powder (equal to 100 mM) was directly added into the mixture at the beginning of the reaction, the DSS concentration was significantly increased to 40 mM within the first 1 h, then slowly increased to 51.5 mM from 1 to 4 h. However, the DSS concentration was gradually decreased after 4 h. The batch addition strategy was performed with the initial addition of 39.4 mg of L-DOPA (20 mM); subsequently, 19.7 mg of L-DOPA (10 mM) was added in batch after each hour. The DSS concentration slowly increased to 45.5 mM from 0 to 8 h, then quickly decreased after 8 h (Figure 5). Based on the batch addition of L-DOPA, enzyme addition in batch at each 3 h was also investigated, and the DSS production trend was similar to that of only L-DOPA addition. Although the highest DSS concentration (47.5 mM) by batch addition of both L-DOPA and enzymes was slightly higher than that of only L-DOPA batch addition (45.5 mM), it was still lower than that of 100 mM L-DOPA without batch addition.

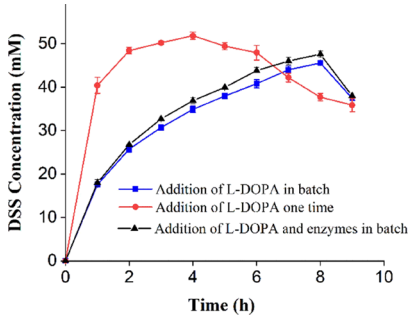

Figure 5. In vitro multi-enzyme cascade synthesis of DSS at 100 mM L-DOPA. Addition of L-DOPA one time: addition of 197 mg of L-DOPA (100 mM) at the beginning of the reaction; addition of L-DOPA in batch: 39.4 mg of L-DOPA (20 mM) was added at the beginning, then 19.7 mg of L-DOPA (10 mM) was added at 1, 2, 3, 4, 5, 6, 7, and 8 h, respectively. Addition of L-DOPA and enzymes in batch: based on the addition of L-DOPA in batch each hour, three enzymes with the total amount of 45 mg were added every 3 h (e.g., 0, 3, and 6 h).

NH_4^+ is one intermediate produced by *Cd*gluD during the multi-enzyme cascade synthesis of DSS. Figure 6a shows that the activity of *Cd*gluD was decreased along with the increasing NH_4^+ concentration and even lost around 80% of its original activity in the presence of 50 mM NH_4^+. This indicates that NH_4^+ accumulation can inhibit the activity of *Cd*gluD, which could no longer provide sufficient α-KG and NADH for the cascade reaction. For cascade reaction with 100 mM L-DOPA, supplement of 10 mM of both α-KG and NADH at 4 h could further enhance the DSS concentration by 16% within the next 1 h (Figure 6b).

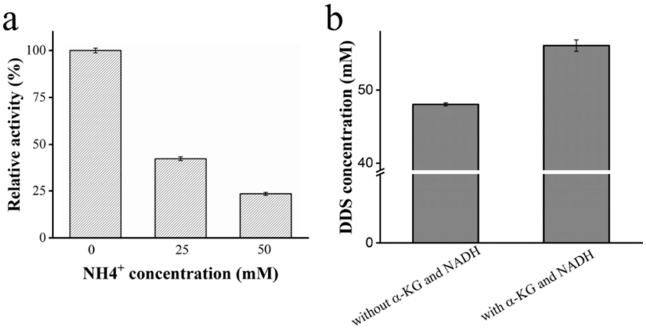

Figure 6. Effect of NH_4^+ concentration on the multi-enzyme cascade reaction. (a) Effect of the NH_4^+ concentration on the activity of *Cd*gluD. (b) Effect of additional α-KG and NADH on DSS production in multi-enzyme cascade reaction. Ten milliliter reaction containing 100 mM L-DOPA, 10 mM NAD^+, 20 mM glutamate, 0.3 U mL^{-1}*Ec*TyrB, 0.2 U mL^{-1}*Lf*D2-HDH, and 0.1 U mL^{-1}*Cd*gluD in 50 mM PBS buffers (pH 7.0) was performed at 35 °C. Values are means of triplicate determinations.

Attempt of NaOH addition was performed to remove the accumulated NH_4^+. As shown in Figure 7, when the pH of mixture was adjusted to 7.5 and 8.0 by adding NaOH after 1 h, the color of the mixture gradually became darker and the yield of DSS gradually decreased as pH increased. In particular, the highest yield of DSS (51.9%) without pH adjustment was achieved at a reaction time of 4 h, whereas that at pH 7.5 (44.7%) and 8.0 (29.3%) was decreased by 13.8 and 43.5%, respectively.

Another approach for NH_4^+ removal was also performed, and 10 g of zeolite was added in the mixture at 1 h. As shown in Figure 7, DSS yields by adding zeolite were significantly enhanced and reached the highest (70.5%) at 4 h, which was 1.36-fold that without zeolite.

DISCUSSION

DSS as a main component in *S. miltiorrhiza* has a high potential for the treatment of cardiovascular diseases. For the

https://doi.org/10.1021/acssynbio.2c00552
ACS Synth. Biol. 2023, 12, 277−286

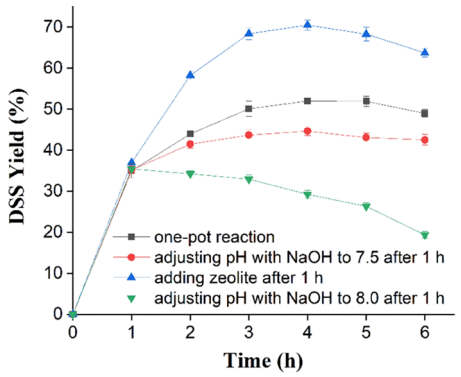

Figure 7. Time course of multi-enzyme reaction by pH adjustment and zeolite addition. pH adjustment was performed by adding NaOH (100 mM) in the reaction mixture to adjust pH to 7.5 and 8.0 after 1 h of reaction. Addition of zeolite was performed by adding 10 g of zeolites in the mixture after 1 h of reaction.

biosynthesis of DSS, an efficient in vitro multi-enzyme cascade route for DSS production from L-DOPA was developed in this study. Compared with chemo-enzymatic methods[17] and whole-cell biocatalytic approaches,[22] this newly designed route displays a number of advantages. First, the production of DSS from L-DOPA by the in vitro one-pot multi-enzyme cascade route is environment-friendly and has less by-products without complex product purification steps.[17,22] Second, compared with the whole-cell biocatalysis process (space–time yield of 1.96 g L^{-1} h^{-1}),[22] this designed in vitro enzymatic pathway presents a higher space–time yield of 6.61 g L^{-1} h^{-1} owing to its faster mass transfer and catalytic efficiency. In addition, the self-sufficient system of the cofactor (NADH) and cosubstrate (α-KG) is achieved within this cascade route. *Cd*gluD catalyzes the dehydrogenation of glutamate to generate α-KG and NADH, providing abundant cosubstrates and cofactors for the reactions catalyzed by *Ec*tyrB and *Lf*D2-HDH. Meanwhile, α-KG can act as an amino acceptor for the synthesis of DPA from L-DOPA by *Ec*TyrB and continuously provides glutamate as the cosubstrate of *Cd*gluD. Compared with the accumulation of byproduct gluconic acid from the reported whole-cell catalysis,[22] this self-sufficient system avoids large accumulation of byproducts and is convenient for the purification of DSS.

In the time-course experiment, an unexpected decrease in the DSS concentration was observed after 2 h (Figure 3c). Meanwhile, the peak area of DPA was gradually increased with increasing reaction time (Figure S3), suggesting DSS was partially oxidized to DPA as reaction proceeds. Therefore, the optimization of reaction conditions was performed to accelerate the yield of DSS and reduce the oxidation of DSS. pH 7.0 was selected for the cascade reaction because of the weak oxidation of DSS at neutrality conditions, even though the optimum reaction pH was determined to be 7.5 (Figure 3b). In the cascade reaction, various enzymes in one pot could have synergistic effects at certain amounts.[44] Here, the ratio of enzyme loadings of *Ec*TyrB, *Lf*D2-HDH, and *Cd*gluD was optimized to be 3:2:1 (Figure 4). To reduce the costs of the cofactor and cosubstrate, small amounts of NAD^+ (5 mM) and glutamate (10 mM) were used instead of expensive NADH and α-KG (Figure 4).

Space–time yield is an important parameter in industrial bioprocesses.[45−47] Although 95% yield of DSS was obtained by the whole-cell biocatalysis,[22] its low space–time yield (1.96 g L^{-1} h^{-1}) and S/C (0.47) is noteworthy. In this in vitro cascade route, the highest space–time yield of 6.61 g L^{-1} h^{-1} was achieved with lower enzyme loadings (S/C = 1.47) (Table 2). Furthermore, although the DSS yield at 100 mM L-DOPA was unexpectedly decreased, this cascade reaction still maintained a higher space–time yield of 2.54 g L^{-1} h^{-1} and S/C of 2.26 than the whole-cell biocatalysis (Table 2).

Most L-DOPA was present as a solid in the mixture because of its low solubility. Considering that high concentrations of L-DOPA may inhibit the cascade catalytic efficiency, the addition of L-DOPA in batch was investigated. However, no positive effect of the batch addition of L-DOPA (Figure 5) was observed in the multi-enzyme cascade reaction for DSS synthesis. Furthermore, to investigate whether insufficient enzymes or enzymatic activities loss are responsible for the low DSS yield at 100 mM L-DOPA, enzyme addition in batch was performed and no significant increase of the DSS yield was observed (Figure 5). Therefore, these results suggest that decreased DSS yield at 100 mM L-DOPA is not ascribed to the substrate inhibition and enzyme shortage in the cascade reaction.

To further understand the reason of reduced DSS yield from elevated concentrations of L-DOPA, the concentration of accumulated NH_4^+ in the cascade reaction mixture was determined to be as high as 43.3 mM (at 4 h). According to the mechanism of this cascade reaction (Figure 8), the

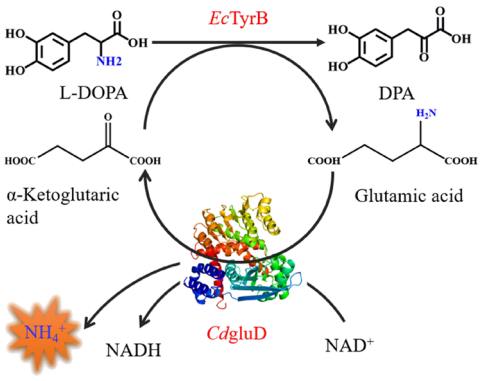

Figure 8. Schematic of the NH4+ transfer pathway in the cascade synthesis of DSS.

amidogen moiety from L-DOPA is transformed to glutamic acid by *Ec*TyrB catalysis, and then NH_4^+ is produced via deamination of glutamic acid by *Cd*gluD. Excess NH_4^+ could hamper the conversion of glutamate to α-KG and NADH by *Cd*gluD because of the reversible reaction,[48] which further inhibited the cascade synthesis of DSS. This hypothesis was further confirmed by the results of severe inhibition of high concentrations of NH_4^+ on *Cd*gluD activity (Figure 6a). Furthermore, supplements of α-KG and NADH could enhance the DSS yield by the cascade reaction (Figure 6b), suggesting that the shortage of α-KG and NADH is mainly responsible for the hindered DSS accumulation. Therefore, efficient strategies for NH_4^+ removal in this cascade route need to be explored. To remove NH_4^+, herein, two approaches of adding NaOH and zeolite were attempted. pH adjustment with NaOH was performed because OH^- could hydrolyze NH_4^+ and release NH_3.[49] However, the yields of DSS at pH 7.5 and 8.0 were gradually decreased (Figure 7), which may be attributed to the oxidation of DSS at alkaline conditions. Absorption using

https://doi.org/10.1021/acssynbio.2c00552
ACS Synth. Biol. 2023, 12, 277−286

zeolite is another effective approach for NH_4^+ removal.[50] Herein, significant enhancement of DSS yield after adding zeolite (Figure 7) further confirms that zeolite is able to reduce the inhibitory effect of accumulated NH_4^+ in this cascade route.

Whole-cell reaction using engineered *E. coli* BL21(DE3) harboring plasmids pRSFDuet1/*Ec*TyrB/*Lf*D2-HDH and pETDuet1/*Cd*gluD was also attempted, but no DSS product was detected (Figure S5b). However, an unknown compound (at a retention time of 8.76 min) was gradually synthesized with decreasing DPA. The reason may be ascribed to an inappropriate ratio of three enzymes (more expression of *Cd*gluD, less expression of *Ec*TyrB and *Lf*D2-HDH) and the effects of other intracellular enzymes (Figure S5a). These results reveal that the synthesis of DSS through this route in the complex intracellular environment needs further optimization.

In summary, a newly designed in vitro one-pot multi-enzyme cascade pathway was successfully constructed for DSS production from L-DOPA for the first time. In this route, a cofactor (NADH) and cosubstrate (α-KG) self-sufficient system was introduced by *Cd*gluD with the addition of cheap glutamate and NAD^+ with low concentrations (10 mM NAD^+ and 20 mM glutamate). Under the optimum reaction conditions, the highest DSS yield reached 98.3% (at 20 mM L-DOPA), and the space−time yield reached 6.61 g L^{-1} h^{-1} (at 40 mM L-DOPA). Additionally, NH_4^+ accumulation was identified to be mainly responsible for the decreased DSS yield with elevated concentrations of L-DOPA. This in vitro multi-enzyme cascade reaction provides a promising alternative route for industrial production of DSS.

MATERIALS AND METHODS

Chemicals. L-DOPA, α-KG, and DSS were purchased from Sigma-Aldrich (Shanghai, China). NADH and NAD^+ were purchased from Sangon (Shanghai Sangon Biotech Co., China). Kanamycin and isopropyl-β-D-thiogalactopyranoside were procured from Generay (Shanghai Generay Biotech Co., China).

Bacterial Strains, Plasmids, and Enzymes. *E. coli* BL21 (DE3) were purchased from Tokyo Chemical Industry (Shanghai, China) and used as hosts for recombinant enzyme expression. Genes encoding *Lf*D2-HDH from *L. frumenti*[43] (GenBank ID ON209401) and *Cd*gluD from *C. difficile*[29,32] (GenBank ID ON209400) were codon-optimized and synthesized by Generay (Shanghai, China). Genes encoding LDHs from other microorganisms (Table S1) were also synthesized by Generay (Shanghai, China). The gene encoding *Ec*TyrB[29,31] was amplified from the DNA genome of *E. coli* BL21 (GenBank ID CP001509.3, from 4174523 to 4175716) using the KOD DNA polymerase with the primers (Table S2). All genes were cloned into plasmid pET-28a(+) between restriction enzyme cutting sites of *Bam* HI and *Xho* I, and recombinant plasmids pET-28a(+)/*Ec-tyrB*, pET-28a(+)/*Lf-hdh*, and pET-28a(+)/*Cd-gluD* were constructed (Figure S4).

Expression and Purification. The constructed recombinant plasmids pET-28a(+)/*Ec-tyrB*, pET-28a(+)/*Lf-hdh*, and pET-28a(+)/*Cd-gluD* were transferred into host strain *E. coli* BL21 (DE3). The recombinant *E. coli* strains were inoculated into 0.7 L of LB medium containing 50 μg/mL kanamycin at 1% ratio (v/v) and then incubated at 37 °C and 200 rpm. When the optical density at 600 nm (OD_{600}) reached 0.6−0.8, expression was induced by adding 0.2 mM isopropyl-β-D-thiogalactopyranoside (IPTG). After further incubation at 16 °C and 200 rpm for 16 h, cells were harvested by centrifugation at 8000 × *g* for 10 min. Then, the cells were resuspended with 20 mM Tris−HCl buffer (pH 7.5, containing 500 mM NaCl and 20 mM imidazole) and disrupted by ultrasonication.

Crude cell extracts were centrifuged for 30 min, and the supernatants were freeze-dried into powder for further investigations. Purification was performed using nickel column affinity chromatography and elution with binding buffer (20 mM Tris−HCl pH 7.5, 500 mM NaCl, and 500 mM imidazole). The eluted fractions were evaluated by SDS-PAGE analysis. The protein concentration was measured using a Thermo Scientific NanoDropTM spectrophotometer (Wilmington, DE, USA).

Enzymatic Activity Assays. Activity of *Ec*TyrB was measured at 30 °C in 50 mM PBS buffer (pH 7.0) containing 5 mM L-DOPA and 5 mM α-KG. The reaction was terminated by adding equal volume of 1 M HCl after incubating for 10 min. The concentration of DPA was measured by HPLC. One unit of *Ec*TyrB activity is defined as the amount of *Ec*TyrB required for the formation of 1 μmol DPA per min.

The activity of *Lf*D2-HDH was measured at 30 °C in 50 mM PBS buffer (pH 7.0) containing 5 mM DPA and 10 mM NADH. The reaction was stopped by adding equal volume of 1 M HCl after 10 min. The concentration of DSS was measured by HPLC. One unit of *Lf*D2-HDH activity is defined as the amount of *Lf*D2-HDH required for the formation of 1 μmol DSS per min.

The activity of *Cd*gluD was measured in 96-well plates at 25 °C using a spectrophotometer. A reaction mixture OF 200 μL contained 10 μL of glutamate (10 mM), 10 μL of NAD^+ (10 mM), 10 μL of *Cd*gluD, and 170 μL of PBS buffer (100 mM, pH 7.0). One unit of *Cd*gluD activity is defined as the amount of *Cd*gluD required for producing 1 μmol NADH per min.

Multi-Enzyme Cascade Synthesis of DSS and Analysis by HPLC and LC−MS. One-pot cascade reaction for biosynthesis of DSS was performed using 10 mL mixture in an Erlenmeyer flask (100 mL), including 50 mM PBS buffer (pH 7.0), 5 mM L-DOPA, 10 mM glutamate, and 10 mM NAD^+. The concentrations of all three enzymes (including purified *Ec*TyrB, *Lf*D2-HDH, and *Cd*gluD) were 0.1 U mL^{-1}. The reaction was conducted at 30 °C, with shaking of 220 rpm, and aliquots of samples were taken periodically at 1, 2, 4, 6, 9, and 12 h.

The production of DSS and DPA and consumption of L-DOPA were measured by HPLC equipped with an Agilent Zorbax SB-C18 column (250 mm × Ø 4.6 mm) at 280 nm. The mobile phase consisted of 100% methanol (solution A), and 0.1% formic acid in water (solution B) was used at a flow rate of 1 mL/min. The gradient elution process was as follows: 0−15 min, 10−100% solution A; 15−20 min, 100% solution A; 20−25 min, 100−10% solution A; and 25−30 min, 10% solution A. The retention times of DSS, DPA, and L-DOPA were determined compared with the standards. The yield was calculated by dividing the concentration of DSS by the initial concentration of L-DOPA.

Reaction products were further identified by the LC−MS analysis using a MALDI SYNAPT Q-TOF Premier mass spectrometer (Waters, USA) equipped with an electrospray ion source performed in the V-Optics negative mode. A BEH C18 column (1.7 μm, 2.1 × 100 mm) was used for liquid chromatogram on an ACQUITY UPLC (Waters, USA).

https://doi.org/10.1021/acssynbio.2c00552
ACS Synth. Biol. 2023, 12, 277−286

Optimization of Conditions for DSS Production. *Temperature and pH.* All reactions were performed in 100 mL Erlenmeyer flask in the following investigation. The effect of temperature and pH on DSS production was investigated. For temperature, a 10 mL reaction was performed at 20−40 °C, containing 10 mM L-DOPA, 10 mM glutamate, 10 mM NAD^+, and 0.1 U mL^{-1} of each enzyme (lyophilized crude enzyme powder) in 50 mM PBS buffer (pH 7.0). For pH, the same reaction system was performed, except various 50 mM PBS buffers of pH 6.0−8.0 were used. The concentration of DSS was measured by HPLC after 2 h of reaction.

Enzyme Loadings of EcTyrB, LfD2-HDH, and CdgluD. Optimization of enzyme loadings (lyophilized crude enzyme powder) was performed at 10 mM L-DOPA. For *Ec*TyrB, enzyme loadings of 0.01−0.3 U mL^{-1} were attempted while the other two enzymes were maintained at 0.1 U mL^{-1}. Under the optimum loading of *Ec*TyrB, *Cd*gluD amounts of 0.01 to 0.2 U mL^{-1} were attempted at 0.1 U mL^{-1}*Lf*D2-HDH. Under the optimum loadings of *Ec*TyrB and *Cd*gluD, *Lf*D2-HDH amounts of 0.01−0.2 U mL^{-1} were conducted. The concentration of DSS was measured as above.

Concentrations of NAD^+ and Glutamate. For NAD^+, the same reaction system containing various concentrations of NAD^+ (0.5−15 mM) was performed at 10 mM L-DOPA and 10 mM glutamate. For glutamate, the same reaction system containing various concentrations of glutamate (0.5−15 mM) was applied at 10 mM L-DOPA and 5 mM NAD^+. DSS concentration was measured as above.

Cascade Reaction at High Concentrations of L-DOPA. A ten milliliter multi-enzyme cascade reaction was conducted at 20−100 mM L-DOPA (39.4−197 mg) and 35 °C, which contained 45 mg of lyophilized crude enzyme powder (0.3 U/mL *Ec*TyrB, 0.2 U/mL *Lf*D2-HDH, and 0.1 U mL^{-1}*Cd*gluD), 20 mM glutamate, and 10 mM NAD^+ in 50 mM PBS buffer (pH 7.0). The concentration of DSS was determined as above.

The addition of L-DOPA in batch was performed as follows: 39.4 mg of L-DOPA (20 mM) was added into the mixture (10 mL) at the beginning of the reaction, and then, 19.7 mg of L-DOPA (10 mM) was added in batch at 1, 2, 3, 4, 5, 6, 7, and 8 h, respectively.

The addition of enzymes in batch was performed as follows. Based on the batch addition of L-DOPA above, 45 mg of lyophilized crude enzyme powder (including 0.3 U mL^{-1}*Ec*TyrB, 0.2 U mL^{-1}*Lf*D2-HDH, and 0.1 U mL^{-1}*Cd*gluD) was added into the mixture (10 mL) at 0, 3, and 6 h, respectively.

The concentration of accumulated NH_4^+ in the cascade reaction mixture was determined by formaldehyde−phenolphthalein titration method.[51]

Whole-Cell Reaction Harboring Plasmids pRSFDuet1/*Ec*TyrB/*Lf*D2-HDH and pETDuet1/*Cd*gluD. The *Ec-tyrB* and *Lf-hdh* genes were cloned into the same plasmid pRSFDuet1 in Multiple Cloning Sites I (MCS I, between *Nco* I and *Hind* III) and MCS II (between *Nde* I and *Xho* I), respectively. The *Cd-gluD* gene was cloned into the plasmid pETDuet1 between *Nco* I and *Hind* III in MCS I. All successfully constructed plasmids were transformed into the same *E. coli* BL21(DE3), and the recombinant *E. coli* harboring both recombinant plasmids pRSFDuet1/*Ec*TyrB/*Lf*D2-HDH and pETDuet1/*Cd*gluD was constructed.

The recombinant *E. coli* strains were inoculated into 0.7 L of LB medium containing 50 μg/mL kanamycin and 100 μg/mL ampicillin at 1% ratio (v/v) and then incubated at 37 °C and 200 rpm. When the optical density at 600 nm (OD_{600}) reached 0.6−0.8, the expression was induced by adding 0.2 mM IPTG. After further incubation at 16 °C and 200 rpm for 16 h, cells were harvested by centrifugation at 8000 × *g* for 10 min. Then, the harvested cells were washed 3 times using 50 mM PBS buffer (pH 7.0) and then were freeze-dried for further investigation.

The whole-cell reaction was performed as follows: a 10 mL reaction mixture containing 100 mM L-DOPA (197 mg), 1 g of freeze-dried cells, 20 mM glutamate, and 10 mM NAD^+ in 50 mM PBS buffer (pH 7.0) was conducted at 35 °C. The sample at various times was determined for the concentration of DSS.

Attempts for Reducing the Effect of NH_4^+ by pH Adjustment and Adding Zeolite. To reduce the accumulated NH_4^+ in the cascade reaction, the approaches of adding NaOH and zeolite were performed, respectively.

pH adjustment by adding NaOH was performed as follows. A ten milliliter multi-enzyme cascade reaction (in 100 mL Erlenmeyer flask) was conducted at 35 °C, which contained 100 mM L-DOPA (197 mg), 45 mg of lyophilized crude enzyme powder (0.3 U/mL *Ec*TyrB, 0.2 U/mL *Lf*D2-HDH, and 0.1 U mL^{-1}*Cd*gluD), 20 mM glutamate, and 10 mM NAD^+ in 50 mM PBS buffer (pH 7.0). After 1 h of cascade reaction, 100 mM NaOH was added in the reaction mixture to adjust pH to 7.5 and 8.0, respectively. The sample at per hour was determined for the concentration of DSS.

The addition of zeolite was performed as follows. A ten milliliter multi-enzyme cascade reaction was performed as described above (pH 7.0 and 35 °C). After 1 h of reaction, 10 g of zeolites were added in the reaction mixture. The sample at per hour was determined for the concentration of DSS.

■ ASSOCIATED CONTENT

Supporting Information

The Supporting Information is available free of charge at https://pubs.acs.org/doi/10.1021/acssynbio.2c00552.

Specific activities of LDHs from different origins; primer sequences used to amplify the *tyrB* gene; SDS-PAGE of LDHs from different microorganisms; HPLC profiles and standard curves of DSS, DPA, and L-DOPA; HPLC analysis of cascade reaction at different times; construction of plasmids pET-28a(+)/*Ec-tyrB*, pET-28a(+)/*Lf-hdh*, and pET-28a(+)/*Cd-gluD*; and analysis of the whole-cell reaction (PDF)

■ AUTHOR INFORMATION

Corresponding Authors

Yu Ji − *Institute of Biotechnology, RWTH Aachen University, Aachen 52074, Germany*; Email: yu.ji@biotec.rwth-aachen.de

Ye Ni − *Key laboratory of Industrial Biotechnology, School of Biotechnology, Jiangnan University, Wuxi 214122, China*; orcid.org/0000-0003-4887-7517; Email: yni@jiangnan.edu.cn

Authors

Ruizhi Han − *Key laboratory of Industrial Biotechnology, School of Biotechnology, Jiangnan University, Wuxi 214122, China; Institute of Biotechnology, RWTH Aachen University, Aachen 52074, Germany*

Ke Gao − *Key laboratory of Industrial Biotechnology, School of Biotechnology, Jiangnan University, Wuxi 214122, China*

https://doi.org/10.1021/acssynbio.2c00552
ACS Synth. Biol. 2023, 12, 277−286

Yulin Jiang − *Key laboratory of Industrial Biotechnology, School of Biotechnology, Jiangnan University, Wuxi 214122, China*

Jieyu Zhou − *Key laboratory of Industrial Biotechnology, School of Biotechnology, Jiangnan University, Wuxi 214122, China*

Guochao Xu − *Key laboratory of Industrial Biotechnology, School of Biotechnology, Jiangnan University, Wuxi 214122, China*

Jinjun Dong − *Key laboratory of Industrial Biotechnology, School of Biotechnology, Jiangnan University, Wuxi 214122, China*

Ulrich Schwaneberg − *Institute of Biotechnology, RWTH Aachen University, Aachen 52074, Germany;* orcid.org/0000-0003-4026-701X

Complete contact information is available at: https://pubs.acs.org/10.1021/acssynbio.2c00552

Author Contributions

#R.H. and K.G. contributed equally to this work.

Author Contributions

Y.N., R.H. conceived and designed research. R.H., K.G., and Y.J. conducted experiments. R.H., K.G., Y.N., and Y.J. analyzed data. R.H. and K.G. performed investigation and wrote the manuscript. Y.N., Y.J., U.S., J.Z., G.X., and J.D. contributed to manuscript revision and reading. All authors read and approved the manuscript.

Notes

The authors declare no competing financial interest.

This article does not contain any studies with human participants or animals performed by any of the author.

■ ACKNOWLEDGMENTS

This work was supported by the National Key Research and Development Program (2021YFC2102700), the National Natural Science Foundation of China (22077054, 31871738), the National First-Class Discipline Program of Light Industry Technology and Engineering (LITE2018-07), and the Program of Introducing Talents of Discipline to Universities (111-2-06).

■ ABBREVIATIONS

DSS, danshengsu; *Ec*TyrB, tyrosine aminotransferase from *Escherichia coli*; *Lf*D2-HDH, D-isomer specific 2-hydroxyacid dehydrogenase from *Lactobacillus frumenti*; *Cd*gluD, glutamate dehydrogenase from *Clostridium difficile*; AADL, L-amino acid deaminase; LDH, lactate dehydrogenase; GDH, glucose dehydrogenase; AroAT, aromatic amino acid aminotransferase; α-KG, α-ketoglutaric acid

■ REFERENCES

(1) Cao, H. Y.; Ding, R. L.; Li, M.; Yang, M. N.; Yang, L. L.; Wu, J. B.; Yang, B.; Wang, J.; Luo, C. L.; Wen, Q. L. Danshensu, a major water-soluble component of *Salvia miltiorrhiza*, enhances the radioresponse for Lewis Lung Carcinoma xenografts in mice. *Oncol. Lett.* **2017**, *13*, 605−612.

(2) Sidoryk, K.; Filip, K.; Cmoch, P.; Laszcz, M.; Cybulski, M. Efficient synthesis and physicochemical characterization of natural danshensu, its S isomer and intermediates thereof. *J. Mol. Struct.* **2018**, *1153*, 135−148.

(3) Yin, Y.; Guan, Y.; Duan, J.; Wei, G.; Zhu, Y.; Quan, W.; Guo, C.; Zhou, D.; Wang, Y.; Xi, M.; Wen, A. Cardioprotective effect of Danshensu against myocardial ischemia/reperfusion injury and inhibits apoptosis of H9c2 cardiomyocytes via Akt and ERK1/2 phosphorylation. *Eur. J. Pharmacol.* **2013**, *699*, 219−226.

(4) Jia, P.; Wang, S.; Xiao, C.; Yang, L.; Chen, Y.; Jiang, W.; Zheng, X.; Zhao, G.; Zang, W.; Zheng, X. The anti-atherosclerotic effect of tanshinol borneol ester using fecal metabolomics based on liquid chromatography-mass spectrometry. *Analyst* **2016**, *141*, 1112−1120.

(5) Qi, J. Y.; Yang, Y. K.; Jiang, C.; Zhao, Y.; Wu, Y. C.; Han, X.; Jing, X.; Wu, Z. L.; Chu, L. Exploring the mechanism of Danshensu in the treatment of doxorubicin-induced cardiotoxicity based on network pharmacology and experimental evaluation. *Front. Cardiovasc. Med.* **2022**, *9*, No. 827975.

(6) Han, B.; Che, X.; Zhao, Y.; Li, C.; He, J.; Lu, Y.; Wang, Z.; Wang, T. Neuroprotective effects of Danshensu in Parkinson's disease mouse model induced by 1-methyl-4-phenyl-1,2,3,6-tetrahydropyridine. *Behav. Pharmacol.* **2019**, *30*, 36−44.

(7) Zhao, G. R.; Zhang, H. M.; Ye, T. X.; Xiang, Z. J.; Yuan, Y. J.; Guo, Z. X.; Zhao, L. B. Characterization of the radical scavenging and antioxidant activities of danshensu and salvianolic acid B. *Food Chem. Toxicol.* **2008**, *46*, 73−81.

(8) Zhou, X.; Chan, S. W.; Tseng, H. L.; Deng, Y.; Hoi, P. M.; Choi, P. S.; Or, P. M.; Yang, J. M.; Lam, F. F.; Lee, S. M.; Leung, G. P.; Kong, S. K.; Ho, H. P.; Kwan, Y. W.; Yeung, J. H. Danshensu is the major marker for the antioxidant and vasorelaxation effects of Danshen (*Salvia miltiorrhiza*) water-extracts produced by different heat water-extractions. *Phytomedicine* **2012**, *19*, 1263−1269.

(9) Zhang, L. J.; Chen, L.; Lu, Y.; Wu, J. M.; Xu, B.; Sun, Z. G.; Zheng, S. Z.; Wang, A. Y. Danshensu has anti-tumor activity in B16F10 melanoma by inhibiting angiogenesis and tumor cell invasion. *Eur. J. Pharmacol.* **2010**, *643*, 195−201.

(10) Yu, C.; Qi, D.; Lian, W.; Li, Q. Z.; Li, H. J.; Fan, H. Y. Effects of danshensu on platelet aggregation and thrombosis: in vivo arteriovenous shunt and venous thrombosis models in rats. *PLoS One* **2014**, *9*, No. e110124.

(11) Li, J.; Chen, Z.; Liao, H.; Zhong, Y.; Hua, J.; Su, M.; Li, J.; Xu, J.; Cui, L.; Cui, Y. Anti-osteogenic effect of Danshensu in ankylosing spondylitis: an *in vitro* study based on integrated network pharmacology. *Front. Pharmacol.* **2021**, *12*, No. 772190.

(12) Chen, Y. W.; Huang, Y. P.; Wu, P. C.; Chiang, W. Y.; Wang, P. H.; Chen, B. Y. The functional vision protection effect of danshensu via dopamine D1 receptors: *in vivo* study. *Nutrients* **2021**, *13*, 978.

(13) Peng, R.; Wu, Q.; Chen, X.; Ghosh, R. Purification of Danshensu from *Salvia miltiorrhiza* extract using graphene oxide-based composite adsorbent. *Ind. Eng. Chem. Res.* **2017**, *56*, 8972−8980.

(14) Wang, B. Q. *Salvia militorrhiza*: Chemical and pharamacological review of a medicinal plant. *J. Med. Plant Res.* **2010**, *4*, 2813−2820.

(15) Wong, H. N. C.; Xu, Z. L.; Chang, H. M.; Lee, C. M. A modified synthesis of (+/−)-beta-aryllactic acids. *Synthesis* **1992**, 793−797.

(16) Demir, A. S.; Emrullahoglu, M.; Pirkin, E.; Akca, N. Darzens reaction of acyl phosphonates with alpha-bromo ketones: selective synthesis of cis- and trans-epoxyphosphonates. *J. Org. Chem.* **2008**, *73*, 8992−8997.

(17) Sayyed, I. A.; Sudalai, A. Asymmetric synthesis of L-DOPA and (R)-selegiline via, OsO4-catalyzed asymmetric dihydroxylation. *Tetrahedron: Asymmetry* **2004**, *15*, 3111−3116.

(18) Yang, L.; Zeng, Q.; Yang, D. J. C. J. o. A. C. Chemoenzymatic Synthesis of Danshensu. *Chin. J. Appl. Chem.* **2016**, *33*, 1073−1078.

(19) Wang, Y. H.; Bai, Y. J.; Fan, T. P.; Zheng, X. H.; Cai, Y. J. Reducing 3,4-dihydroxyphenylpyruvic acid to D-3,4-dihydroxyphenyllactic acid via a coenzyme nonspecific d-lactate dehydrogenase from *Lactobacillus reuteri*. *J. Appl. Microbiol.* **2018**, *125*, 1739−1748.

(20) Min, K.; Park, K.; Park, D. H.; Yoo, Y. J. Overview on the biotechnological production of L-DOPA. *Appl. Microbiol. Biotechnol.* **2015**, *99*, 575−584.

(21) Findrilk, Z.; Poijanac, M.; Vasic-Racki, D. Modelling and optimization of the (R)-(+)-3,4-dihydroxyphenyllactic acid production catalyzed with D-lactate dehydrogenase from *Lactobacillus*

leishmannii using genetic algorithm. *Chem. Biochem. Eng. Q.* **2005**, *19*, 351−358.
(22) Xiong, T.; Jiang, J.; Bai, Y.; Fan, T. P.; Zhao, Y.; Zheng, X.; Cai, Y. Biosynthesis of D-danshensu from L-DOPA using engineered *Escherichia coli* whole cells. *Appl. Microbiol. Biotechnol.* **2019**, *103*, 6097−6105.
(23) You, C.; Shi, T.; Li, Y.; Han, P.; Zhou, X.; Zhang, Y. P. An *in vitro* synthetic biology platform for the industrial biomanufacturing of myo-inositol from starch. *Biotechnol. Bioeng.* **2017**, *114*, 1855−1864.
(24) Meng, D. D.; Wei, X. L.; Bai, X.; Zhou, W.; You, C. Artificial *in vitro* synthetic enzymatic biosystem for the one-pot sustainable biomanufacturing of glucosamine from starch and inorganic ammonia. *ACS Catal.* **2020**, *10*, 13809−13819.
(25) Morgado, G.; Gerngross, D.; Roberts, T. M.; Panke, S. Synthetic biology for cell-free biosynthesis: fundamentals of designing novel *in vitro* multi-enzyme reaction networks. *Adv. Biochem. Eng./Biotechnol.* **2018**, *162*, 117−146.
(26) You, C.; Zhang, Y. H. P. Biomanufacturing by *in vitro* biosystems containing complex enzyme mixtures. *Process Biochem.* **2017**, *52*, 106−114.
(27) Lopez-Gallego, F.; Schmidt-Dannert, C. Multi-enzymatic synthesis. *Curr. Opin. Chem. Biol.* **2010**, *14*, 174−183.
(28) Ricca, E.; Brucher, B.; Schrittwieser, J. H. Multi-enzymatic cascade reactions: overview and perspectives. *Adv. Synth. Catal.* **2011**, *353*, 2239−2262.
(29) France, S. P.; Hepworth, L. J.; Turner, N. J.; Flitsch, S. L. Constructing biocatalytic cascades: *in vitro* and *in vivo* approaches to de novo multi-enzyme pathways. *ACS Catal.* **2017**, *7*, 710−724.
(30) Cong, X.; Li, X.; Li, S. Crystal structure of the aromatic-amino-acid aminotransferase from *Streptococcus mutans*. *Acta Crystallogr., Sect. F: Struct. Biol. Commun.* **2019**, *75*, 141−146.
(31) Prabhu, P. R.; Hudson, A. O. Identification and partial characterization of an L-Tyrosine Aminotransferase (TAT) from *Arabidopsis thaliana*. *Biochem. Res. Int.* **2010**, *2010*, No. 549572.
(32) Lee, E. J.; Facchini, P. J. Tyrosine aminotransferase contributes to benzylisoquinoline alkaloid biosynthesis in opium poppy. *Plant Physiol.* **2011**, *157*, 1067−1078.
(33) Matelska, D.; Shabalin, I. G.; Jablonska, J.; Domagalski, M. J.; Kutner, J.; Ginalski, K.; Minor, W. Correction to: Classification, substrate specificity and structural features of D-2-hydroxyacid dehydrogenases: 2HADH knowledgebase. *BMC Psychiatry* **2019**, *19*, 221.
(34) Foster, J. W.; Park, Y.; Penfound, T.; Fenger, T.; Spector, M. J. Regulation of NAD metabolism in Salmonella typhimurium: molecular sequence analysis of the bifunctional nadR regulator and the nadA-pnuC operon. *J. Bacteriol.* **1990**, *172*, 4187−4196.
(35) Bastos, F. d. M.; dos Santos, A. G.; Jones, J.; Oestreicher, E. G.; Pinto, G. F.; Paiva, L. M. C. Three different coupled enzymatic systems for in situ regeneration of NADPH. *Biotechnol. Tech.* **1999**, *13*, 661−664.
(36) Nidetzky, B.; Haltrich, D.; Schmidt, K.; Schmidt, H.; Weber, A.; Kulbe, K. D. Simultaneous enzymatic synthesis of mannitol and gluconic acid: II. Development of a continuous process for a coupled NAD (H)-dependent enzyme system. *Biocatal. Biotransform.* **1996**, *14*, 47−65.
(37) Jiang, W.; Fang, B. Construction and evaluation of a novel bifunctional phenylalanine−formate dehydrogenase fusion protein for bioenzyme system with cofactor regeneration. *J. Ind. Microbiol. Biotechnol.* **2016**, *43*, 577−584.
(38) Tang, C.-D.; Zhang, Z.-H.; Shi, H.-L.; Xie, Y.-L.; Yang, T.-T.; Lu, Y.-F.; Zhang, S.-P.; Bai, F.-H.; Kan, Y.-C.; Yao, L.-G. Directed evolution of formate dehydrogenase and its application in the biosynthesis of L-phenylglycine from phenylglyoxylic acid. *Mol. Catal.* **2021**, *513*, No. 111666.
(39) Li, C.; Jia, P.; Bai, Y.; Fan, T. P.; Zheng, X.; Cai, Y. Efficient synthesis of hydroxytyrosol from l-3,4-dihydroxyphenylalanine using engineered *Escherichia coli* whole cells. *J. Agric. Food Chem.* **2019**, *67*, 6867−6873.
(40) Powell, J. T.; Morrison, J. F. The purification and properties of the aspartate aminotransferase and aromatic-amino-acid amino-transferase from *Escherichia coli*. *Eur. J. Biochem.* **1978**, *87*, 391−400.
(41) Anderson, B. M.; Anderson, C. D.; Van Tassell, R. L.; Lyerly, D. M.; Wilkins, T. D. Purification and characterization of *Clostridium difficile* glutamate dehydrogenase. *Arch. Biochem. Biophys.* **1993**, *300*, 483−488.
(42) Heo, J.; Hamada, M.; Cho, H.; Weon, H. Y.; Kim, J. S.; Hong, S. B.; Kim, S. J.; Kwon, S. W. Weissella cryptocerci sp. nov., isolated from gut of the insect *Cryptocercus kyebangensis*. *Int. J. Syst. Evol. Microbiol.* **2019**, *69*, 2801−2806.
(43) Sun, Z.; Harris, H. M.; McCann, A.; Guo, C.; Argimon, S.; Zhang, W.; Yang, X.; Jeffery, I. B.; Cooney, J. C.; Kagawa, T. F.; Liu, W.; Song, Y.; Salvetti, E.; Wrobel, A.; Rasinkangas, P.; Parkhill, J.; Rea, M. C.; O'Sullivan, O.; Ritari, J.; Douillard, F. P.; Paul Ross, R.; Yang, R.; Briner, A. E.; Felis, G. E.; de Vos, W. M.; Barrangou, R.; Klaenhammer, T. R.; Caufield, P. W.; Cui, Y.; Zhang, H.; O'Toole, P. W. Expanding the biotechnology potential of lactobacilli through comparative genomics of 213 strains and associated genera. *Nat. Commun.* **2015**, *6*, 8322.
(44) Siedentop, R.; Claaßen, C.; Rother, D.; Lütz, S.; Rosenthal, K. J. C. Getting the most out of enzyme cascades: Strategies to optimize in vitro multi-enzymatic reactions. *Catalysts* **2021**, *11*, 1183.
(45) Wechselberger, P.; Sagmeister, P.; Engelking, H.; Schmidt, T.; Wenger, J.; Herwig, C. Efficient feeding profile optimization for recombinant protein production using physiological information. *Bioprocess Biosyst. Eng.* **2012**, *35*, 1637−1649.
(46) Bayer, B.; Dalmau Diaz, R.; Melcher, M.; Striedner, G.; Duerkop, M. Digital twin application for model-based doe to rapidly identify ideal process conditions for space-time yield optimization. *Processes* **2021**, *9*, 1109.
(47) Sinner, P.; Herwig, C.; Kager, J. Time scale analysis and optimization of a continuous microbial bioprocess. *Comput. Aided Chem. Eng.* **2020**, *48*, 1603−1608.
(48) Plaitakis, A.; Kalef-Ezra, E.; Kotzamani, D.; Zaganas, I.; Spanaki, C. The glutamate dehydrogenase pathway and its roles in cell and tissue biology in health and disease. *Biology* **2017**, *6*, 11.
(49) Zuo, X.; He, H.; Yang, Y.; Yan, C.; Zhou, Y. Study on control of $NH4^+$-N in surface water by photocatalytic. *IOP Conf. Ser. Earth Environ. Sci.* **2018**, *108*, No. 022031.
(50) Muscarella, S. M.; Badalucco, L.; Cano, B.; Laudicina, V. A.; Mannina, G. Ammonium adsorption, desorption and recovery by acid and alkaline treated zeolite. *Bioresour. Technol.* **2021**, *341*, No. 125812.
(51) Qing-Lan, H. U.; Fang, J. L. Amount of formaldehyde on the determination of nitrogen in $(NH_4)_2SO_4$ by formaldehyde method. *J. Hubei Univ. Educ.* **2013**, *30*, 4−5.

https://doi.org/10.1021/acssynbio.2c00552
ACS Synth. Biol. 2023, 12, 277−286